DOI: 10.1002/ejic.200800058

# Hydrothermal Synthesis, Structural Characterisations, and Photoluminescence Properties of Four Inorganic-Organic Hybrid Compounds in the Indium/Gallium Iodate Family

**Xiaomin Liu,[a] Guanghua Li,[a] Bin Hu,[a] Yang Yu,[a] Yawei Hu,[a] Minghui Bi,[a] Zhan Shi,*[a] and Shouhua Feng[a]**

**Keywords:** Hydrothermal synthesis / Hybrid material / Indium iodate / Gallium iodate / Crystal structure / Photoluminescence

Four inorganic-organic hybrid compounds with the formulae $In_2(IO_3)_6(H_2O)$(2,2′-bipy)·$H_2O$ (**1**), $In_2(IO_3)_6(H_2O)$(1,10-phen)·$H_2O$ (**2**), $Ga(IO_3)_3$(2,2′-bipy)·$HIO_3$ (**3**) and $Ga(IO_3)_3$(1,10-phen)·$H_2O$ (**4**) were hydrothermally synthesised at 100 °C over 7 d and subsequently characterised by single-crystal X-ray diffraction. The bidentate diamine ligands 2,2′-bipy and 1,10-phen in the In/I/O system give rise to the compounds $In_2(IO_3)_6(H_2O)$(2,2′-bipy)·$H_2O$ and $In_2(IO_3)_6(H_2O)$(1,10-phen)·$H_2O$ which crystallise in the monoclinic space group $P2_1/c$. Using the same bidentate diamine ligands, namely 2,2′-bipy and 1,10-phen, in the Ga/I/O system led to the formation of $Ga(IO_3)_3$(2,2′-bipy)·$HIO_3$ and $Ga(IO_3)_3$(1,10-phen)·$H_2O$ which crystallise in the monoclinic space group $P2_1/n$. Both, $In_2(IO_3)_6(H_2O)$(2,2′-bipy)·$H_2O$ and $In_2(IO_3)_6(H_2O)$(1,10-phen)·$H_2O$ possess 2D layered structures, with the former consisting of $[In(H_2O)(IO_3)_5]^{2-}$ clusters and $[In(IO_3)$(2,2′-bipy)$]^{2+}$ chains and the latter consisting of $[In(H_2O)(IO_3)_5]^{2-}$ clusters and $[In(IO_3)$(1,10-phen)$]^{2+}$ chains. Compound $Ga(IO_3)_3$(2,2′-bipy)·$HIO_3$ is a 1D ribbon built up from $[IO_3]$ pyramids, $[GaO_4N_2]$ octahedra and distinct $[I_2O_6]$ units and featuring interesting left and right helical chains. Compound $Ga(IO_3)_3$-(1,10-phen)·$H_2O$ has a 1D chain-like structure constructed from the alternation of $[GaO_4N_2]$ octahedra and $[IO_3]$ pyramids. By comparatively studying the photoluminescence properties of these compounds, we may conclude that the photoluminescence originates from ligand-centred π-π* transitions. The synthesised products were further characterised by powder X-ray diffraction, thermogravimetric analysis, IR spectroscopy, ICP and elemental analysis.



## Introduction

The design and synthesis of inorganic-organic hybrid materials have provoked significant interest owing to their rich structural chemistry and potential applications in catalysis, biology, optical and electromagnetic functions.[1–4] The structures of a number of such materials have been reported and these show various architectures with 1D, 2D and 3D connections between inorganic and organic species.[5–7] A study of the literature of inorganic-organic hybrid materials shows that 1,10-phen and 2,2′-bipy are extensively used organic ligands for achieving various open framework structures and the inorganic skeletons focus on metal phosphate,[8–10] arsenate,[11–12] sulfate,[13–14] germinate,[15] phosphite[16] and selenite functions.[17] In order to extend the field of the system, one could search other tetrahedral or pseudotetrahedral coordination groups and one might focus on iodate. The iodate anion, with a geometry similar to that of selenite, contains stereochemically active lone pairs of electrons and has a propensity for forming low-dimensional structures that are often noncentrosymmetric (NCS).

Materials with NCS structures are of great interest due to their potential nonlinear optical, piezoelectric, pyroelectric and ferroelectric properties.[18–22] Considering these properties, one would expect the iodate pyramid to be able to play a role similar to that of the selenite pyramid which constructs the inorganic framework and brings some new properties to hybrid materials. However, due to their strongly oxidising nature ($E^{\theta}_{IO_3/I_2}$ = 1.209 V), only some simple metal iodates have been reported so far such as $Co(IO_3)_2$, $Cu(IO_3)_2$, $M(IO_3)_3{\cdot}nH_2O$ (M = Ce–Lu), $A[VO_2(IO_3)_2]$ (A = K, Rb), $A[(VO)_2(IO_3)_3O_2]$ (A = $NH_4$, Rb, Cs), $AMoO_3(IO_3)$ (A = K, Rb, Cs), *RE*$(MoO_2)(IO_3)_4$-(OH) (*RE* = Nd, Sm, Eu), $Ce(IO_3)_6(OH)$, $UO_2(IO_3)_2(H_2O)$, $Ag_4(UO_2)_4(IO_3)_2(IO_4)_2O_2$, $K_2[(UO_2)_2(VO)_2(IO_6)_2O]{\cdot}H_2O$, $Cf(IO_3)_3$, $BaTi(IO_3)_6$, $LaTi(IO_3)_5$, $In(IO_3)_3$ and $Ga(IO_3)_3$.[23–36] Our group has initiated an investigation of the hydrothermal synthesis of inorganic-organic hybrid materi-

[a] State Key Laboratory of Inorganic Synthesis & Preparative Chemistry, College of Chemistry, Jilin University, Changchun 130012, People's Republic of China
Fax: +86-431-85168624
E-mail: zshi@mail.jlu.edu.cn

Supporting information for this article is available on the WWW under http://www.eurjic.org/ or from the author.

  

als in the M/P/O, M/Se/O system.[5–7,17,37–40] With a view to the comparability of selenite and iodate, we have been researching metal iodate systems in order to create new materials and extend the field of open-framework hybrid materials. We have successfully synthesised three hybrid copper iodates: $(2,2'\text{-bipy})_2Cu_2(IO_3)_3\cdot 1.5Cl\cdot 0.5H_3O\cdot 4H_2O\cdot xI_2$ ($x \approx 0.19$) with potentially large void volumes,[41] $[Cu_3(2,2'\text{-bipy})_3Cl_3(IO_3)_2]\cdot I_{1.5}$ and $[Cu(2,2'\text{-bipy})(H_2O)(IO_3)_2]\cdot(H_2O)_2$ as well as two hybrid vanadium iodates: $(VO_2)$(1,10-phen)$(IO_3)$ and $(VO_2)(2,2'\text{-bipy})(IO_3)$. Considering the coordination variety of indium and gallium, we set out to exploit some new hybrid compounds in the In/Ga/I/O system and obtained two indium iodates, $In_2(IO_3)_6(H_2O)(2,2'\text{-bipy})\cdot H_2O$ and $In_2(IO_3)_6(H_2O)(1,10\text{-phen})\cdot H_2O$, and two gallium iodates, $Ga(IO_3)_3(2,2'\text{-bipy})\cdot HIO_3$ and $Ga(IO_3)_3(1,10\text{-phen})\cdot H_2O$. To the best of our knowledge, these are the first organic-inorganic hybrid indium/gallium iodates. Herein, we report the hydrothermal synthesis, X-ray crystal structure, thermal stabilities as well as the photoluminescence properties of these four compounds.

## Results and Discussion

### Synthesis

The reaction of an In or Ga source with $I_2O_5$ and the organic ligands 1,10-phen or 2,2′-bipy in aqueous media at 100 °C leads to the formation of the four above mentioned organic-inorganic hybrid indium/gallium iodates. With regards to the option of organic ligands, we had to use some organic amines that are not easily oxidised due to the strongly oxidising nature of $I_2O_5$. Organic amines are oxidised easily in the presence of strong oxidants. A primary amine is oxidised easily to give a mixture of products, a secondary amine yields the hydroxylation product while a tertiary amine gives an *N*-oxide as the sole product. In all cases the function of the organic ligand is lost.[42] There are two reasons why we chose 1,10-phen and 2,2′-bipy. One is their structural stability, namely that they are not oxidised easily and the other is our synthetic experience in using 1,10-phen and 2,2′-bipy to achieve various open inorganic-organic frameworks.[5–7,16–17,37–41] On the basis of our group's study of the V/Cu/I/O system, we applied these ligands to the In/Ga/I/O system and isolated the four hybrid indium/gallium iodates. Even though we used the relatively stable 1,10-phen and 2,2′-bipy, they could still be oxidised when the reaction temperature exceeded 120 °C.

### Crystal Structure of $In_2(IO_3)_6(H_2O)(2,2'\text{-bipy})\cdot H_2O$ (1)

Single-crystal structural analysis revealed that $In_2(IO_3)_6(H_2O)(2,2'\text{-bipy})\cdot H_2O$ possesses a 2D layered structure. An ORTEP drawing of the asymmetric unit of $In_2(IO_3)_6(H_2O)(2,2'\text{-bipy})\cdot H_2O$ is shown in Figure 1 and the compound crystallises in the monoclinic space group $P2_1/c$. There are two crystallographically distinct In atoms and six crystallographically distinct I atoms in an asymmetric unit. Of the two unique In atoms, In(1) and In(2) are both octahedrally coordinated, the difference being that In(1) exhibits an octahedral geometry of $[InO_4N_2]$, shares four oxygen atoms with the adjacent iodate groups [In(1)–O(1) 2.107 Å, In(1)–O(2) 2.236 Å, In(1)–O(3) 2.222 Å, In(1)–O(4) 2.134 Å] and two nitrogen atoms with the organic ligand 2,2′-bipy [In(1)–N(1) 2.253 Å, In(1)–N(2) 2.249 Å] whereas In(2) exhibits an octahedral geometry of $[InO_6]$, coordinated by five oxygen atoms from the adjacent iodate groups [In(2)–O(5) 2.125 Å, In(2)–O(6) 2.135 Å, In(2)–O(7) 2.126 Å In(2)–O(8) 2.135 Å, In(2)–O(9) 2.189 Å] and one oxygen atom from a water molecule [In(2)–O(10) 2.144 Å]. Of the six unique I atoms, I(1), I(2) and I(3) each offer two oxygen atoms to bridge the adjacent indium atoms and have one terminal oxygen atom with bond lengths in the range of 1.788–1.832 Å and I–O–I angles in the range of 95.71–102.63°. I(4), I(5) and I(6) each share one oxygen atom with the adjacent indium atoms and possess two terminal oxygen atoms with bond lengths ranging from 1.775–1.853 Å and I–O–I angles ranging from 94.11–99.05°. It was observed that the I–O bond lengths for the oxygen atoms bound to the indium atoms are longer than those of the terminal oxo groups.

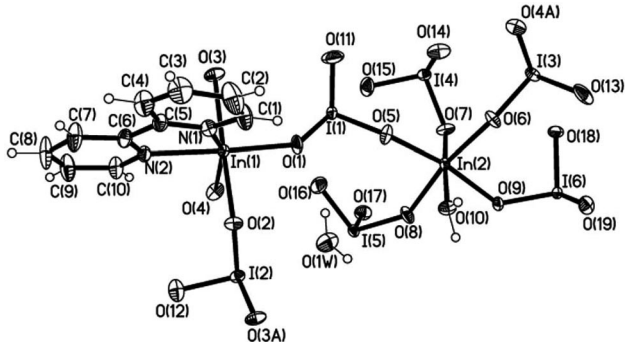


Figure 1. Asymmetric unit of $In_2(IO_3)_6(H_2O)(2,2'\text{-bipy})\cdot H_2O$.

The alternation of $[InO_4N_2]$ octahedra, $[InO_6]$ octahedra and $[IO_3]$ pyramids results in 2D infinite layers which consist of two structural building units. One is the infinite $[In(IO_3)(2,2'\text{-bipy})]^{2+}$ chain and the other is the $[In(H_2O)(IO_3)_5]^{2-}$ cluster. As can be seen in part a of Figure 2, the chains can be described as indium iodate lines constructed from the corner sharing of $[InO_4N_2]$ octahedra and $[IO_3]$ pyramids and attended by 2,2′-bipy molecules. The anion cluster is composed of one $[InO_6]$ octahedron and five $[IO_3]$ pyramids (see Figure 2, b). The anion clusters bridge the adjacent chains into 2D layers along the *b* direction. Figure 2 (c) shows the arrangement of 2D layers containing 12-ring apertures. The adjacent layers are further connected through very strong π-π interactions between the ligands with an average interplanar distance of 3.55 Å, indicating significant attractive intermolecular aromatic interactions (see Figure 2, d).

  

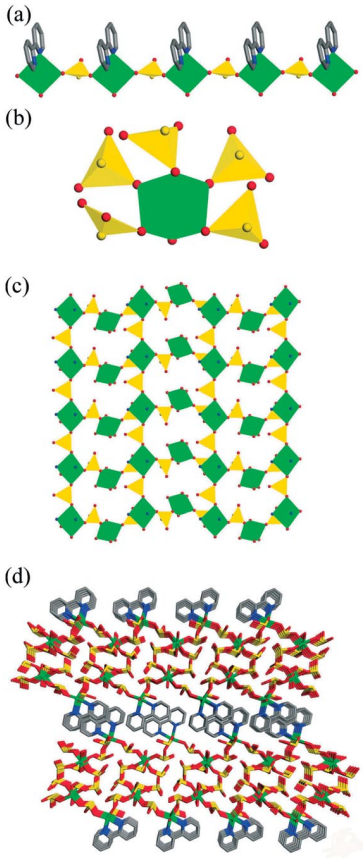


Figure 2. (a) View of the $[In(IO_3)(2,2'\text{-bipy})]^{2+}$ chain. (b) View of the $[In(H_2O)(IO_3)_5]^{2-}$ cluster. (c) View of the layered structure of compound **1**. Organic ligands of $[In(IO_3)(2,2'\text{-bipy})]^{2+}$ chains and terminal iodate groups of $[In(H_2O)(IO_3)_5]^{2-}$ clusters are omitted for clarity. (d) The packing of compound **1** projected along the *b* axis. The following colours correspond to the respective atoms: indium, green; iodine, yellow; oxygen, red; nitrogen, blue; carbon, grey.

### Crystal Structure of $In_2(IO_3)_6(H_2O)(1,10\text{-phen})\cdot H_2O$ (2)

Compared with $In_2(IO_3)_6(H_2O)(2,2'\text{-bipy})\cdot H_2O$, $In_2(IO_3)_6(H_2O)(1,10\text{-phen})\cdot H_2O$ has a similar layered structure but a different unit cell. Compound $In_2(IO_3)_6(H_2O)(1,10\text{-phen})\cdot H_2O$ crystallises in the monoclinic space group $P2_1/c$. As shown in Figure 3, it also has two crystallographically distinct In atoms and six crystallographically distinct I atoms in an asymmetric unit.

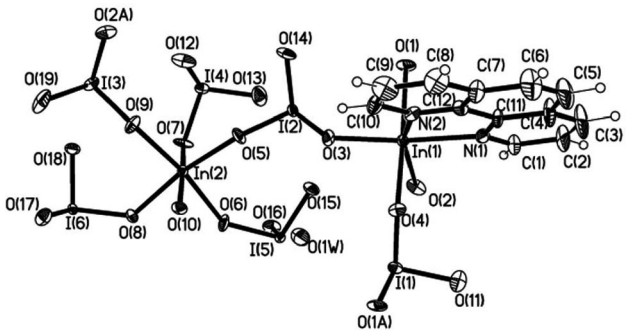


Figure 3. Asymmetric unit of $In_2(IO_3)_6(H_2O)(1,10\text{-phen})\cdot H_2O$.

The coordination environments of In and I in compound $In_2(IO_3)_6(H_2O)(1,10\text{-phen})\cdot H_2O$ are similar to those of $In_2(IO_3)_6(H_2O)(2,2'\text{-bipy})\cdot H_2O$ with In–O bond lengths ranging from 2.113–2.229 Å, I–O bond lengths varying from 1.772–1.853 Å and I–O–I angles in the range of 93.1–102.6°. Structural analysis indicates that like $In_2(IO_3)_6(H_2O)(2,2'\text{-bipy})\cdot H_2O$, $In_2(IO_3)_6(H_2O)(1,10\text{-phen})\cdot H_2O$ also possesses a 2D-layered structure but consists of infinite $[In(IO_3)(1,10\text{-phen})]^{2+}$ chains (see Figure 4, a) and $[In(H_2O)(IO_3)_5]^{2-}$ clusters. As can be seen from part b of Figure 4, the adjacent layers are further connected through very strong π-π interactions between 1,10-phen molecules. The interplanar distance between the adjacent ligands is about 3.50 Å, also indicating significant attractive intermolecular aromatic interactions. Interestingly, in the asymmetric units of $In_2(IO_3)_6(H_2O)(2,2'\text{-bipy})\cdot H_2O$ and $In_2(IO_3)_6(H_2O)(1,10\text{-phen})\cdot H_2O$, the 2,2′-bipy and 1,10-phen organic ligands selectively coordinate to In(1) atoms, so the coordination environments of indium atoms in $In_2(IO_3)_6(H_2O)(2,2'\text{-bipy})\cdot H_2O$ and $In_2(IO_3)_6(H_2O)(1,10\text{-phen})\cdot H_2O$ are of two different types. The In(1) atoms show $[InO_4N_2]$ octahedral geometry and the In(2) atoms take the form of $[InO_6]$ octahedra. $[InO_4N_2]$ octahedra and $[InO_6]$ octahedra share corners with $[IO_3]$ pyramids to form chains and clusters, respectively. The clusters connect the chains into 2D layers. To the best of our knowledge, these are the first inorganic-organic hybrid indium iodates.

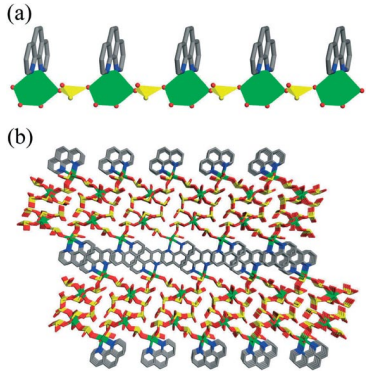


Figure 4. (a) View of the $[In(IO_3)(1,10\text{-phen})]^{2+}$ chain. (b) The packing of compound **2** projected along the *b* axis. The following colours correspond to the respective atoms: indium, green; iodine, yellow; oxygen, red; nitrogen, blue; carbon, grey.

### Crystal Structure of $Ga(IO_3)_3(2,2'\text{-bipy})\cdot HIO_3$ (3)

Considering the coordination similarity of In and Ga, we replaced indium with gallium (but using the same organic ligands, 2,2′-bipy and 1,10-phen) and obtained the compounds $Ga(IO_3)_3(2,2'\text{-bipy})\cdot HIO_3$ and $Ga(IO_3)_3(1,10\text{-phen})\cdot H_2O$, respectively. Interestingly, these two compounds are different from $In_2(IO_3)_6(H_2O)(2,2'\text{-bipy})\cdot H_2O$ and $In_2(IO_3)_6(H_2O)(1,10\text{-phen})\cdot H_2O$ in their crystal structures. Moreover, $Ga(IO_3)_3(2,2'\text{-bipy})\cdot HIO_3$ and $Ga(IO_3)_3(1,10\text{-phen})\cdot H_2O$ are distinct from each other. An ORTEP drawing of the asymmetric unit of $Ga(IO_3)_3(2,2'\text{-bipy})\cdot HIO_3$ (see

  

Figure 5) indicates that it crystallises in the monoclinic space group $P2_1/n$ with a unit cell content of 29 non-hydrogen atoms and all atoms in general positions.

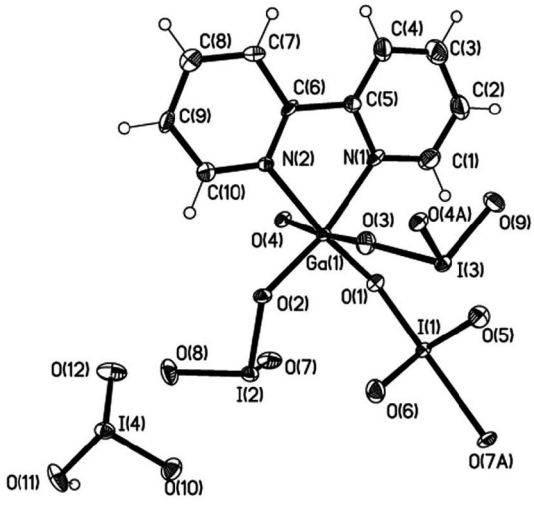


Figure 5. Asymmetric unit of $Ga(IO_3)_3(2,2'\text{-bipy})\cdot HIO_3$.

The asymmetric unit contains one crystallographically distinct Ga atom and four crystallographically distinct I atoms. The gallium site in the asymmetric unit exhibits an octahedral geometry and has the formula $[GaO_4N_2]$, shares four oxygen atoms with the adjacent iodate groups [Ga(1)–O(1) 1.935 Å, Ga(1)–O(2) 1.955 Å, Ga(1)–O(3) 1.966 Å, Ga(1)–O(4) 1.995 Å] and two nitrogen atoms with the 2,2′-bipy ligand [Ga(1)–N(1) 2.089 Å, Ga(1)–N(2) 2.089 Å]. Of the four unique I atoms, I(1) exhibits an $[IO_4]$ polyhedral geometry, shares one oxygen atom with the $[GaO_4N_2]$ octahedron [I(1)–O(1) 1.861 Å], one oxygen atom with the adjacent $[IO_3]$ pyramid [I(1)–O(7) 2.43 Å] and possesses two terminal oxygen atoms [I(1)–O(5) 1.790 Å, I(1)–O(6) 1.794 Å]. I(2) exhibits an $[IO_3]$ pyramidal geometry, shares one oxygen atom with the $[GaO_4N_2]$ octahedron [I(2)–O(2) 1.83 Å], one oxygen atom with the adjacent $[IO_4]$ polyhedron [I(2)–O(7) 1.815 Å] and possesses one terminal oxygen atom [I(2)–O(8) 1.783 Å]. I(3) takes the form of an $[IO_3]$ unit, shares two oxygen atoms with the $[GaO_4N_2]$ octahedron [I(3)–O(3) 1.815 Å, I(3)–O(4) 1.834 Å] and possesses one terminal oxygen atom [I(3)–O(9) 1.786 Å]. I(4) belongs to the iodate unit with bond lengths ranging from 1.769–1.859 Å and bond angles in the range of 95.6–101.0°.

It can also be observed that the I–O bond lengths for oxygen atoms bound to gallium atoms are longer than those of the terminal oxo groups. As shown in Figure 6 (a), compound **3** has a 1D ribbon structure constructed from $[GaO_4N_2]$ octahedra, $[IO_3]$ pyramids and $[I_2O_6]^{2-}$ units. In connectivity terms, the $[I(3)O_3]$ pyramid bridges the adjacent $[GaO_4N_2]$ octahedra to form a chain, whereas the other two $[I(1)O_3]$ and $[I(2)O_3]$ pyramids share one oxygen atom to form $[I_2O_6]^{2-}$ units which bridge the adjacent chains into ribbons. It is noteworthy that the $[I_2O_6]^{2-}$ unit is rare in metal iodates. The I–O bond lengths in the unit ranging from 1.783–2.43 Å are consistent with those of previously reported iodates.[43–49] Distinctively, $Ga(IO_3)_3(1,10\text{-phen})\cdot H_2O$ possesses right and left helical chains consisting of $[GaO_4N_2]$ octahedra and $[I_2O_6]^{2-}$ units. As can be seen from part b of Figure 6, $[I_2O_6]^{2-}$ units share oxygen atoms with $[GaO_4N_2]$ octahedra to connect the adjacent gallium iodate chains into ribbons in such a way that a helix is created that follows the $2_1$ screw axis along the *b* axis. The left and right handed helical chains are strictly alternating due to the symmetry. Figure 6 (c) shows the arrangement of 1D ribbons projected along the *b* direction. The adjacent ribbons are further connected through the very strong π-π interactions between the ligands. The interplanar distance between the adjacent ligands is about 3.32 Å, indicating significant attractive intermolecular aromatic interactions. Iodate groups reside in the inter-ribbon space, forming hydrogen bonds with each other with the OH···O distances being 2.57 Å.

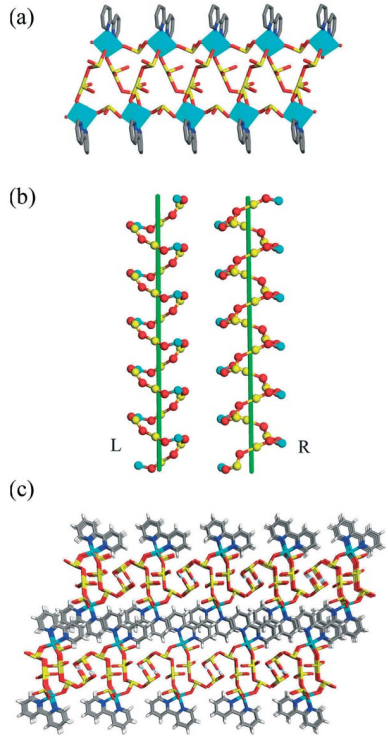


Figure 6. (a) View of the 1D ribbon of compound **3** along the *b* axis. (b) View of the left and right helical chains along the *b* axis. (c) The packing of compound **3** projected along the *b* axis. The following colours correspond to the respective atoms: gallium, light blue; iodine, yellow; oxygen, red; nitrogen, blue; carbon, grey.

## Crystal Structure of $Ga(IO_3)_3(1,10\text{-phen})\cdot H_2O$ (4)

Compound $Ga(IO_3)_3(1,10\text{-phen})\cdot H_2O$ is obtained by replacing 2,2′-bipy with 1,10-phen. As seen in Figure 7, the asymmetric unit contains 28 non-hydrogen atoms. In the asymmetric unit are one crystallographically distinct Ga atom and three crystallographically distinct I atoms. The gallium site in the asymmetric unit exhibits an octahedral geometry as a $[GaO_4N_2]$ unit, shares four oxygen atoms with the adjacent iodate groups [Ga(1)–O(1) 2.016 Å, Ga(1)–O(2) 1.944 Å, Ga(1)–O(3) 1.893 Å, Ga(1)–O(4)

  

1.985 Å] and two nitrogen atoms with the 1,10-phen ligand [Ga(1)–N(1) 2.080 Å, Ga(1)–N(2) 2.088 Å]. Of the three unique I atoms, I(1) has an [$IO_3$] pyramidal geometry, shares two oxygen atoms with the [$GaO_4N_2$] octahedron and has one terminal oxygen atom. I(2) and I(3) also take the form of an [$IO_3$] pyramidal geometry but each shares one oxygen atom with a [$GaO_4N_2$] octahedron and has two terminal oxygen atoms. The bond lengths range from 1.790–1.835 Å and the I–O–I angles range from 94.67–101.32°.

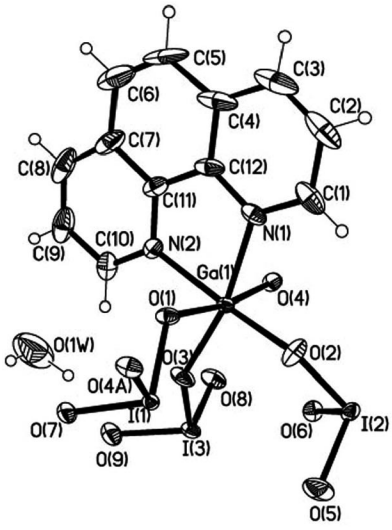


Figure 7. Asymmetric unit of $Ga(IO_3)_3(1,10\text{-phen})\cdot H_2O$.

Compound $Ga(IO_3)_3(1,10\text{-phen})\cdot H_2O$ can be described as gallium iodate chains coordinated with bidentate 1,10-phen ligands. The inorganic chains are constructed from corner-sharing [$GaO_4N_2$] octahedra and [$IO_3$] pyramids (see Figure 8,a). As can be seen from Figure 8 (b), the adjacent inorganic chains are further connected through very strong π-π interactions between the ligands to form pseudo 2D layers. The overlapping distance between the adjacent ligands is about 3.06 Å. Water molecules reside in the interlayer space, forming hydrogen bonds with the host framework with OH···O distances ranging from 2.84–3.01 Å. These perform a certain function of stabilising the structure of $Ga(IO_3)_3(1,10\text{-phen})\cdot H_2O$, thus leading to a pseudo 3D structure.

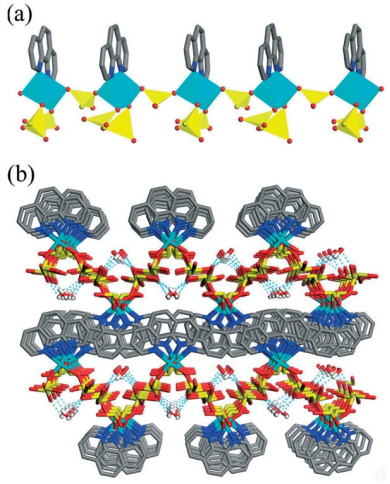


Figure 8. (a) View of the 1D chain of compound **4** along the *c* axis. (b) The packing of compound **4** projected along the *c* axis. The following colours correspond to the respective atoms: gallium, light blue; iodine, yellow; oxygen, red; nitrogen, blue; carbon, gray.

## X-ray Powder Diffraction and Thermal Analysis

The experimental and simulated X-ray powder diffraction patterns of these four compounds are in good agreement with each other (see Supporting Information), substantiating the phase purity of the synthesised products. The difference in reflection intensity is probably caused by the preferred orientation effect in the powder sample. The absence of some reflections might be a result of their relatively low intensity. Thermal analyses for all the compounds were performed in air from 40 to 800 °C as can be seen from Figure 9. The TG curves for $In_2(IO_3)_6(H_2O)(2,2'\text{-bipy})\cdot H_2O$ show that the initial weight loss in the temperature range 280–380 °C is due to the decomposition of 2,2′-bipy and the removal of water molecules (weight loss: exp. 14.75%, calcd: 13.05%). Over the range 430–680 °C, the weight loss should correspond to the condensation of the [$IO_3$] group into $I_2O_5$ and the volatilisation of iodine groups (weight loss: exp. 52.86%, calcd. 51.79%). The TG curve for $In_2(IO_3)_6(H_2O)(1,10\text{-phen})\cdot H_2O$ shows that the initial weight loss in the temperature range 310–380 °C is due to the decomposition of 1,10-phen and loss of water molecules (weight loss: exp. 14.64%, calcd. 13.38%). Further, the loss in weight can be observed from 460 to 630 °C and this can be attributed to the condensation of the [$IO_3$] group into $I_2O_5$ and the volatilisation of iodine groups (weight loss: exp. 51.84%, calcd. 50.96%). Beyond 630 °C, the weight becomes constant owing to the formation of metal oxide. The TG curve for $Ga(IO_3)_3(2,2'\text{-bipy})\cdot HIO_3$ indicates a weight loss of 36.15% (calcd. 35.83%) in the range 240–380 °C, corresponding to the decomposition of the 2,2′-bipy ligands and the removal of iodate groups. Over the range 480–

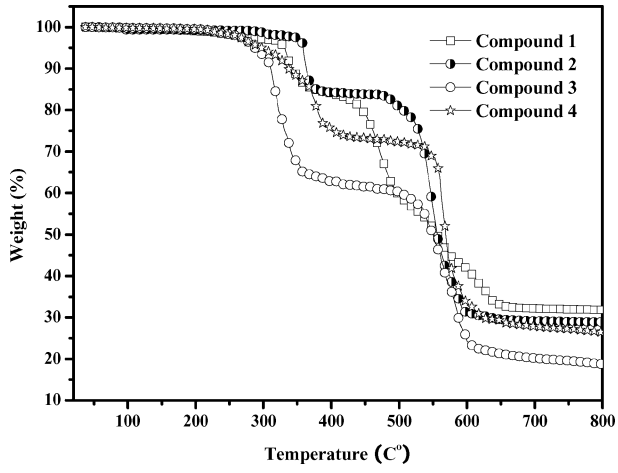


Figure 9. TG curves of four compounds.

  

630 °C, the weight loss of 42.34% should correspond to the sublimation of iodine (calcd. 41.12%). The TG curve for $Ga(IO_3)_3(1,10\text{-phen})\cdot H_2O$ indicates two weight loss steps. The first step in the range of 220–390 °C is due to the decomposition of the 1,10-phen ligands and the removal of water molecules (weight loss: exp. 25.86%, calcd: 24.98%). The second step ranging from 530–640 °C can be attributed to the condensation of the $[IO_3]$ group into $I_2O_5$ and the volatilisation of iodine groups (weight loss: exp. 48.59%, calcd. 48.06%). Beyond 640 °C the weight becomes constant due to the formation of metal oxide.

### Luminescence Properties

The UV/Vis absorption spectra of the four compounds and organic ligands are given in Figure 10. On the basis of the absorption spectra of the free ligands as well as those of the closely related four compounds, we assigned the dominant absorption bands in the 220–400 nm region to the intra-ligand π-π* transition of the ligands.

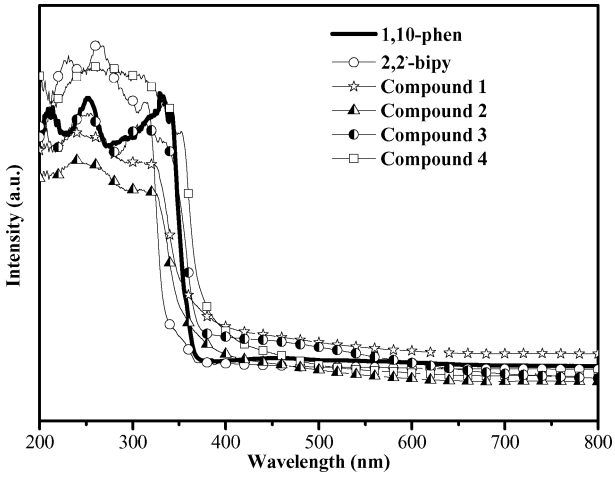


Figure 10. UV spectra of the four compounds and ligands.

The absorption spectra of these four compounds are red-shifted relative to those of the ligands and this may be due to perturbation of the π-π* transition of the ligands by the metal atom. Having the same organic ligand but different inorganic frameworks [compounds $In_2(IO_3)_6(H_2O)(2,2'\text{-bipy})\cdot H_2O$ and $Ga(IO_3)_3(2,2'\text{-bipy})\cdot HIO_3$ or compounds $In_2(IO_3)_6(H_2O)(1,10\text{-phen})\cdot H_2O$ and $Ga(IO_3)_3(1,10\text{-phen})\cdot H_2O$] or the same inorganic framework but different organic ligands [compounds $In_2(IO_3)_6(H_2O)(2,2'\text{-bipy})\cdot H_2O$ and $In_2(IO_3)_6(H_2O)(1,10\text{-phen})\cdot H_2O$] leads to diverse photoluminescence properties. Figure 11 shows the emission spectra of these four compounds in the solid state at room temperature, together with those for 2,2′-bipy and 1,10-phen. When illuminated at a wavelength of 234 nm, $In_2(IO_3)_6(H_2O)(2,2'\text{-bipy})\cdot H_2O$ displays a strong fluorescence emission band centred at 418 nm, whereas $Ga(IO_3)_3(2,2'\text{-bipy})\cdot HIO_3$ exhibits an emission band at 420 nm, slightly red-shifted in comparison to $In_2(IO_3)_6(H_2O)(2,2'\text{-bipy})\cdot H_2O$. This may be due to the better overlap between adjacent 2,2′-bipy ligands in $Ga(IO_3)_3(2,2'\text{-bipy})\cdot HIO_3$ compared with $In_2(IO_3)_6(H_2O)(2,2'\text{-bipy})\cdot H_2O$, increasing the π-π* stacking interactions of $Ga(IO_3)_3(2,2'\text{-bipy})\cdot HIO_3$ and leading to the red-shift observation.[50] For $In_2(IO_3)_6(H_2O)(1,10\text{-phen})\cdot H_2O$, an emission band in the range of 424 nm can be observed, red-shifted relative to that of $In_2(IO_3)_6(H_2O)(2,2'\text{-bipy})\cdot H_2O$ despite it having the same inorganic framework. The probable explanation is that the effect of replacing 2,2′-bipy with 1,10-phen leads to this red-shift phenomena. Compound $Ga(IO_3)_3(1,10\text{-phen})\cdot H_2O$ shows an emission band at 426 nm, red-shifted relative to $In_2(IO_3)_6(H_2O)(1,10\text{-phen})\cdot H_2O$. This may also be due to the better overlap between adjacent 1,10-phen ligands of $Ga(IO_3)_3(1,10\text{-phen})\cdot H_2O$ compared with $In_2(IO_3)_6(H_2O)(1,10\text{-phen})\cdot H_2O$. Because these four compounds are thermally stable and insoluble in common polar and nonpolar solvents, they might be promising candidates for further application as light emitting materials.

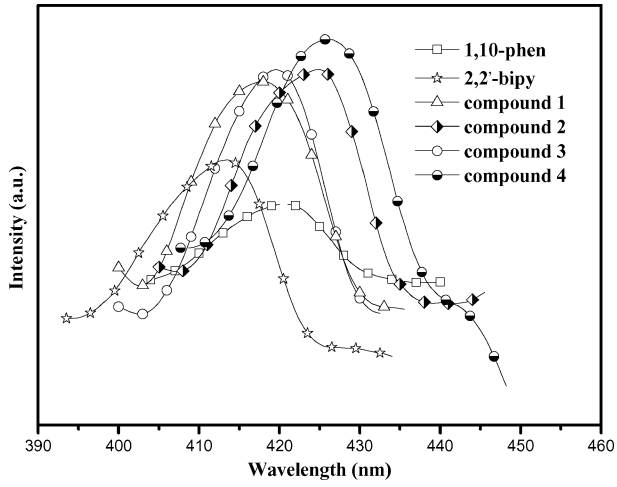


Figure 11. Fluroescence spectra at room temperature for the four compounds and ligands.

## Conclusions

Two indium iodates, namely $In_2(IO_3)_6(H_2O)(2,2'\text{-bipy})\cdot H_2O$ (**1**) and $In_2(IO_3)_6(H_2O)(1,10\text{-phen})\cdot H_2O$ (**2**) as well as two gallium iodates, $Ga(IO_3)_3(2,2'\text{-bipy})\cdot HIO_3$ (**3**) and $Ga(IO_3)_3(1,10\text{-phen})\cdot H_2O$ (**4**) have been hydrothermally synthesised and characterised by single-crystal X-ray diffraction. Considering the various coordination environments of In and Ga, we initially intended to synthesise organic amine templated indium/gallium iodates possessing potentially useful properties. However, due to the strongly oxidising nature of the iodate group, we chose some relatively stable organic amines such as 1,10-phen and 2,2′-bipy. Finally we obtained the four compounds above which are rare examples of inorganic-organic hybrid metal iodates. Importantly, comparison of the photoluminescence properties of these four compounds presents some distinct qualities, providing an approach for obtaining different solid-

  

state photoluminescence emitting materials by optimising the inorganic framework or the attendant organic ligand. It is evident that the hydrothermal technique offers a powerful method for the synthesis of modified metal oxide structures and the isolation of new inorganic-organic hybrid materials.

## Experimental Section

**Synthesis and Characterisation:** Chemicals were used as obtained without further purification. Elemental analyses were performed on a Perkin–Elmer 2400 elemental analyser. Inductively coupled plasma (ICP) analysis was carried out on a Perkin–Elmer Optima 3300DV ICP instrument. Thermogravimetric analysis (TGA) was carried out on a Perkin–Elmer DTA 1700 differential thermal analyser. X-ray powder diffraction (XRD) data were collected on a Siemens D5005 diffractometer with Cu-$K_\alpha$ radiation ($\lambda$ = 1.5418 Å). The infrared (IR) spectra were recorded within the 400–4000 $cm^{-1}$ region on a Nicolet Impact 410 FTIR spectrometer using KBr pellets. Fluorescence spectra were measured on a Perkin–Elmer LS 55 luminescence spectrometer equipped with a 450-W xenon lamp. The diffuse-reflectance UV/Vis spectra for powdered samples were obtained on a Perkin–Elmer Lambda 20 UV/Vis spectrometer equipped with an integrating sphere, using $BaSO_4$ as the background material.

**Synthesis of $In_2(IO_3)_6(H_2O)$(2,2′-bipy)·$H_2O$ (1):** $I_2O_5$ (0.5 g, 1.5 mmol) was dissolved in water (5.0 mL, 166 mmol) whereupon $In(NO_3)_3$·20.5$H_2O$ (0.19 g, 0.5 mmol) and 2,2′-bipy (0.085 g, 0.5 mmol) were added with stirring to form a solution. The solution was stirred for a further 30 min. The final reaction mixture was transferred to a sealed Teflon™-lined steel autoclave and heated at 100 °C for 7 d. Colourless needles suitable for X-ray diffraction were isolated in 80% yield. $In_2(IO_3)_6(H_2O)$(2,2′-bipy)·$H_2O$ (1471.26): calcd. In 15.61, C 8.16, H 0.82, N 1.9; found In 15.81, C 8.34, H 0.96, N 2.13. IR (KBr): $\tilde{\nu}$ = 3528.2 (m), 3444.4 (m), 3217.7 (w), 3104.4 (w), 3026.8 (w), 1934.7 (w), 1612.5 (m), 1481.2 (m), 1439.9 (s), 1314.4 (m), 1254.8 (w), 1165.2 (w), 1033.9 (m), 950.2 (w), 789.3 (m), 729.6 (m) $cm^{-1}$.

**Synthesis of $In_2(IO_3)_6(H_2O)$(1,10-phen)·$H_2O$ (2):** $I_2O_5$ (0.333 g, 1 mmol) was dissolved in water (5.0 mL, 166 mmol) whereupon $In(NO_3)_3$·20.5$H_2O$ (0.19 g, 0.5 mmol) and 1.10-phen (0.1 g, 0.5 mmol) were added with stirring to form a solution. After being stirred for 30 min, the final reaction mixture was heated in a sealed Teflon™-lined steel autoclave at 100 °C for 7 d. Colourless blocks suitable for X-ray diffraction were isolated in 30% yield. $In_2(IO_3)_6(H_2O)$(1,10-phen)·$H_2O$(1495.28): calcd. In 15.36, C 9.63, H 0.8, N 1.87; found In 15.53, C 9.78, H 0.95, N 2.01. IR (KBr): $\tilde{\nu}$ = 3528.2 (m), 3444.4 (m), 3235.6 (w), 1588.7 (w), 1523.3 (m), 1374.1 (w), 1153.2 (w), 1111.5 (w), 801.3 (m), 735.5 (w), 574.6 (m) $cm^{-1}$.

**Synthesis of $Ga(IO_3)_3$(2,2′-bipy)·$HIO_3$ (3):** A solution of $I_2O_5$ (0.333 g, 1.0 mmol), GaO(OH) (0.1 g, 1 mmol), 2,2′-bipy (0.085 g, 0.5 mmol) and $H_2O$ (3 mL) was stirred briefly before being heated to 100 °C for 7 d. Colourless sheets suitable for X-ray diffraction were isolated in 40% yield. $Ga(IO_3)_3$(2,2′-bipy)·$HIO_3$(926.51): calcd. Ga 7.52, C 12.95, H 0.97, N 3.02; found Ga 7.48, C 12.62, H 0.85, N 2.95. IR (KBr): $\tilde{\nu}$ = 3528.2 (m), 3444.4 (m), 3235.6 (w), 1624.6 (w), 1582.9 (m), 1517.1 (w), 1433.7 (w), 1379.9 (w), 1147.3 (w), 1105.5 (w), 759.3 (m), 729.7 (m), 562.5 (m) $cm^{-1}$.

**Synthesis of $Ga(IO_3)_3$(1,10-phen)·$H_2O$ (4):** A solution of $I_2O_5$ (0.5 g, 1.5 mmol), GaO(OH) (0.1 g, 1 mmol), 1,10-phen (0.1 g, 0.5 mmol) and $H_2O$ (3 mL) was stirred briefly before being heated to 100 °C for 7 d. Colourless blocks suitable for X-ray diffraction were isolated in 60% yield. $Ga(IO_3)_3$(1,10-phen)·$H_2O$ (792.64): calcd. Ga 8.79, C 18.17, H 1.26, N 3.53; found Ga 8.52, C 18.05, H 1.09, N 3.34. IR (KBr): $\tilde{\nu}$ = 3528.2 (m), 3444.4 (m), 3235.6 (w), 1612.5 (w), 1588.8 (w), 1517.1 (w), 1427.7 (w), 1385.9 (w), 1147.3 (w), 1111.5 (w), 759.3 (m), 723.4 (m), 562.5 (m) $cm^{-1}$.

**Structural Determination:** Crystals were carefully selected for X-ray diffraction analysis. The intensity data were collected on a Rigaku RAXIS-RAPID single-crystal diffractometer equipped with a narrow-focus, 5.4 kW sealed-tube X-ray source (graphite-monochromated Mo-$K_\alpha$ radiation with $\lambda$ = 0.71073 Å) at a temperature of 20 ± 2 °C. Data processing was accomplished using the PROCESS-AUTO processing program. All of the structures were solved by direct methods using SHELXS-97 and refined by full-matrix least-squares techniques against $F^2$ using the SHELXTL-97 crystallographic software package.[51] Details of the final refinement are given in Table 1.

CCDC-671282 (for **1**), -671283 (for **2**), -671284 (for **3**) and -671285 (for **4**) contain the supplementary crystallographic data for this paper. These data can be obtained free of charge from the Cambridge Crystallographic Data Centre via www.ccdc.cam.ac.uk/data_request/cif.

Table 1. Crystallographic data for compounds **1**–**4**.

| | **1** | **2** | **3** | **4** |
|---|---|---|---|---|
| Empirical formula | $C_{10}H_{12}In_2I_6N_2O_{20}$ | $C_{12}H_{12}In_2I_6N_2O_{20}$ | $C_{10}H_9GaI_4N_2O_9$ | $C_{12}H_{10}GaI_3N_2O_{10}$ |
| $M_r$ | 1471.26 | 1495.28 | 926.51 | 792.64 |
| $T$ [K] | 293(2) | 293(2) | 293(2) | 293(2) |
| $\lambda$ [Å] | 0.71073 | 0.71073 | 0.71073 | 0.71073 |
| Crystal system | monoclinic | monoclinic | monoclinic | monoclinic |
| Space group | $P2_1/c$ | $P2_1/c$ | $P2_1/n$ | $P2_1/c$ |
| $a$ [Å] | 19.091(4) | 20.296(4) | 15.253(3) | 13.567(3) |
| $b$ [Å] | 7.1020(14) | 7.1040(14) | 6.4904(13) | 11.108(2) |
| $c$ [Å] | 19.518(4) | 19.458(4) | 19.614(4) | 12.986(3) |
| $\beta$ [°] | 104.49(3) | 107.63(3) | 112.19(3) | 115.34(3) |
| $V$ [Å$^3$] | 2562.2(9) | 2673.3(9) | 1798.0(6) | 1768.6(6) |
| $Z$ | 4 | 4 | 4 | 4 |
| $D_{calcd.}$ [g $cm^{-3}$] | 3.814 | 3.715 | 3.423 | 2.977 |
| $\mu$ [$mm^{-1}$] | 9.125 | 8.749 | 8.469 | 6.852 |
| $R_1[I > 2\sigma(I)]$[a] | 0.0207 | 0.0350 | 0.0409 | 0.0191 |
| $wR_2[I > 2\sigma(I)]$ | 0.0413 | 0.0646 | 0.0912 | 0.0368 |

[a] $R_1 = \Sigma||F_o| - |F_c||/\Sigma|F_o|$. $wR_2 = \{\Sigma[w(F_o^2 - F_c^2)^2]/\Sigma[w(F_o^2)]^2\}^{1/2}$.

  

**Supporting Information** (see also the footnote on the first page of this article): IR spectra and X-ray diffraction patterns.

## Acknowledgments

This work was supported by the National Natural Science Foundation of China (No. 20121103, 20671040 and 20601010), the 863 Program and the Fok Ying Tung Education Foundation.

[1] G. Férey, *Chem. Mater.* **2001**, *13*, 3084–3098 and references cited therein.
[2] P. J. Hagrman, D. Hagrman, J. Zubieta, *Angew. Chem. Int. Ed.* **1999**, *38*, 2638–2684 and references cited therein.
[3] A. K. Cheetham, G. Ferey, T. Loiseau, *Angew. Chem. Int. Ed.* **1999**, *38*, 3268 and references cited therein.
[4] M. Eddaoudi, D. B. Moler, H. Li, B. Chen, T. M. Reineke, O. M. Yaghi, *Acc. Chem. Res.* **2001**, *34*, 319–330.
[5] Z. Shi, S. Feng, S. Gao, L. Zhang, G. Yang, J. Hua, *Angew. Chem. Int. Ed.* **2000**, *39*, 2325–2327.
[6] Z. Shi, D. Zhang, S. Feng, G. Li, Z. Dai, W. Fu, X. Chen, *J. Chem. Soc., Dalton Trans.* **2002**, 1873–1876.
[7] Z. Shi, L. Zhang, G. Zhu, G. Yang, J. Hua, H. Ding, S. H. Feng, *Chem. Mater.* **1999**, *11*, 3565–3570.
[8] S. Mandal, S. K. Pati, M. A. Green, S. Natarajan, *Chem. Mater.* **2005**, *17*, 638–643.
[9] W. J. Chang, Y. C. Jiang, S. L. Wang, K. H. Lii, *J. Solid State Chem.* **2006**, *179*, 3059–3063.
[10] C. Qin, L. Xu, Y. G. Wei, X. L. Wang, F. Y. Li, *Inorg. Chem.* **2003**, *42*, 3107–3110.
[11] E. Burkholder, S. Wright, V. Golub, J. Zubieta, *Inorg. Chem.* **2003**, *42*, 7460–7471.
[12] Y. Hou, S. T. Wang, E. H. Shen, D. R. Xiao, C. W. Hu, *J. Mol. Struct.* **2004**, *689*, 81–86.
[13] V. M. Hultgren, A. M. Bond, A. G. Wedd, *J. Chem. Soc., Dalton Trans.* **2001**, 1076–1081.
[14] M. I. Khan, S. Cevik, R. J. Doedens, *Chem. Commun.* **2001**, 1930–1931.
[15] S. T. Zheng, J. Zhang, G. Y. Yang, *Inorg. Chem. Commun.* **2004**, *7*, 861–863.
[16] Z. Shi, G. H. Li, D. Zhang, J. Hua, S. H. Feng, *Inorg. Chem.* **2003**, *42*, 2357–2361.
[17] Z. M. Dai, Z. Shi, G. H. Li, D. Zhang, S. H. Feng, *Inorg. Chem.* **2003**, *42*, 7396–7402.
[18] P. S. Halasyamani, K. P. Poeppelmeier, *Chem. Mater.* **1998**, *10*, 2753–2769.
[19] K. Nassau, J. W. Shiever, B. E. Prescott, *J. Solid State Chem.* **1973**, *7*, 186–204.
[20] S. C. Abrahams, R. C. Sherwood, J. L. Bernstein, K. Nassau, *J. Solid State Chem.* **1973**, *7*, 205–212.
[21] C. Svensson, S. C. Abrahams, J. L. Bernstein, *J. Solid State Chem.* **1981**, *36*, 195–204.
[22] J. G. Bergman, G. D. Boyd, A. Ashkin, S. K. Kurtz, *J. Appl. Phys.* **1969**, *40*, 2860–2863.
[23] B. Bentria, D. Benbertal, A. Mosset, I. Gautier-Luneau, *Solid State Sci.* **2006**, *8*, 1466–1472.
[24] R. Liminga, S. C. Abrahams, J. L. Bernstein, *J. Chem. Phys.* **1975**, *62*, 4388–4392.
[25] X. Chen, H. Xue, X. Chang, H. Zang, W. Xiao, *J. Alloys Compd.* **2006**, *415*, 261–265.
[26] D. Phanon, A. Mosset, I. Gautier-Luneau, *J. Mater. Chem.* **2007**, *17*, 1123–1130.
[27] R. E. Sykora, L. Deakin, A. Mar, T. E. Albrecht-Schmitt, *Chem. Mater.* **2004**, *16*, 1343–1349.
[28] R. E. Sykora, K. M. Ok, P. S. Halasyamani, T. E. Albrecht-Schmitt, *Chem. Mater.* **2002**, *14*, 2741–2749.
[29] R. E. Sykora, T. E. Albrecht-Schmitt, *Inorg. Chem.* **2003**, *42*, 2179–2181.
[30] T. C. Shekee, R. E. Sykora, K. M. Ok, P. S. Halasyamani, T. E. Albercht-Schmitt, *Inorg. Chem.* **2003**, *42*, 457–462.
[31] R. E. Sykora, Z. Assfa, R. G. Haire, *Inorg. Chem.* **2006**, *45*, 475–477.
[32] J. Ling, T. E. Albrecht-Schmitt, *Inorg. Chem.* **2007**, *46*, 346–347.
[33] K. M. Ok, P. S. Halasyamani, *Inorg. Chem.* **2005**, *44*, 2263–2271.
[34] A. C. Bean, C. F. Campana, O. Kwon, T. E. Albrecht-Schmitt, *J. Am. Chem. Soc.* **2001**, *123*, 8806–8810.
[35] R. E. Sykora, K. M. Ok, P. S. Halasyamani, T. E. Albrecht-Schmitt, *J. Am. Chem. Soc.* **2002**, *124*, 1951.
[36] N. Ngoa, K. Kalachnikovaa, Z. Assefa, R. G. Hairec, R. E. Sykora, *J. Solid State Chem.* **2006**, *179*, 3824–3830.
[37] Z. Shi, S. H. Feng, L. Zhang, G. Yang, J. Hua, *Chem. Mater.* **2000**, *12*, 2930–2934.
[38] Z. M. Dai, Z. Shi, G. H. Li, X. B. Chen, S. H. Feng, *J. Solid State Chem.* **2003**, *172*, 205–211.
[39] Z. Shi, D. Zhang, G. H. Li, S. H. Feng, *J. Solid State Chem.* **2003**, *172*, 464–470.
[40] W. S. Fu, Z. Shi, D. Zhang, G. H. Li, S. H. Feng, *J. Solid State Chem.* **2003**, *174*, 11–17.
[41] G. H. Li, Z. Shi, X. M. Liu, Z. M. Dai, L. Gao, S. H. Feng, *Inorg. Chem.* **2004**, *43*, 8224–8226.
[42] P. K. Bansal, *A Textbook of Organic Chemistry*, 4th ed., New Age International Ltd. Press, **2003**.
[43] N. W. Alcock, *Acta Crystallogr., Sect. B* **1972**, *28*, 2783–2785.
[44] E. Coquet, J. M. Crettez, J. Pannetier, J. Bouillot, J. C. Damien, *Acta Crystallogr., Sect. B* **1983**, *39*, 408–410.
[45] B. W. Lucas, *Acta Crystallogr., Sect. C* **1984**, *40*, 1989–1991.
[46] C. Svensson, K. Stahl, *J. Solid State Chem.* **1988**, *77*, 112–119.
[47] K. Stahl, M. Szafranski, *Acta Chem. Scand.* **1992**, *46*, 1146–1150.
[48] K. M. Ok, P. S. Halasyamani, *Inorg. Chem.* **2005**, *44*, 9353–9359.
[49] K. M. Ok, P. S. Halasyamani, *Angew. Chem. Int. Ed.* **2004**, *43*, 5489–5491.
[50] D. Miller, D. Swenson, E. Gillan, *J. Am. Chem. Soc.* **2004**, *126*, 5372–5373.
[51] G. M. Sheldrick, *SHELXL*, version 5.1, Siemens Industrial Automation, Inc., Madison, WI, **1997**.

Received: January 18, 2008
Published Online: April 21, 2008

  